



# Morphodynamics of the Kulsi River Basin in the northern front of Shillong Plateau: Exhibiting episodic inundation and channel migration

WATINARO IMSONG<sup>1,2,\*</sup> , SWAPNAMITA CHOUDHURY<sup>1</sup>, SARAT PHUKAN<sup>2</sup> and BHAGAWAT PRAN DUARAH<sup>2</sup>

<sup>1</sup>Wadia Institute of Himalayan Geology, Dehradun 248 001, India.

<sup>2</sup>Department of Geological Sciences, Gauhati University, Guwahati 781 014, India.

\*Corresponding author. e-mail: [imsongnar@gmail.com](mailto:imsongnar@gmail.com)

MS received 15 March 2017; revised 23 May 2017; accepted 12 June 2017; published online 14 February 2018

The present study is undertaken in the Kulsi River valley, a tributary of the Brahmaputra River that drains through the tectonically active Shillong Plateau in northeast India. Based on the fluvial geomorphic parameters and Landsat satellite images, it has been observed that the Kulsi River migrated 0.7–2 km westward in its middle course in the past 30 years. Geomorphic parameters such as longitudinal profile analysis, stream length gradient index ( $SL$ ), ratio of valley floor width to valley height ( $Vf$ ), steepness index ( $k_s$ ) indicate that the upstream segment of the Kulsi River is tectonically more active than the downstream segment which is ascribed to the tectonic activities along the Guwahati Fault.  $^{14}C$  ages obtained from the submerged tree trunks of the Chandubi Lake, which is located in the central part of the Kulsi River catchment suggests inundation (high lake levels) during  $160 \pm 50$  AD,  $970 \pm 50$  AD,  $1190 \pm 80$  AD and  $1520 \pm 30$  AD, respectively. These periods broadly coincide with the late Holocene strengthened Indian Summer Monsoon (ISM), Medieval Warm Period (MWP) and the early part of the Little Ice Age (LIA). The debris which clogged the course of the river in the vicinity of the Chandubi Lake is attributed to tectonically induced increase in sediment supply during high magnitude flooding events.

**Keywords.** Shillong Plateau; geomorphic indices; Kulsi River; channel migration; Chandubi Lake; Indian summer monsoon.

## 1. Introduction

The Shillong Plateau (SP) is a north dipping, detached block of the peninsular India which is separated by the Garo–Rajmahal depression (Evans 1964). The north to northeastward counter clockwise movement of the Indian plate around the eastern Himalayan syntaxis (England and Bilham 2015) makes this plateau a geodynamically active

block south of the Himalayan Frontal Thrust. The SP has witnessed the Great Earthquake of 12 June 1897 (Mw 8.3), along with several significant earthquakes, such as the 10 January 1869 (Mw 7.3), 8 July 1918 (Mw 7.1), 9 September 1923 (Mw 7.1), 3 July 1930 (Mw 7) and 23 October 1943 (Mw 7.1), with epicenters located around the Shillong–Mikir Hills (Dasgupta 2011). The southern margin of the plateau is delimited by Dauki

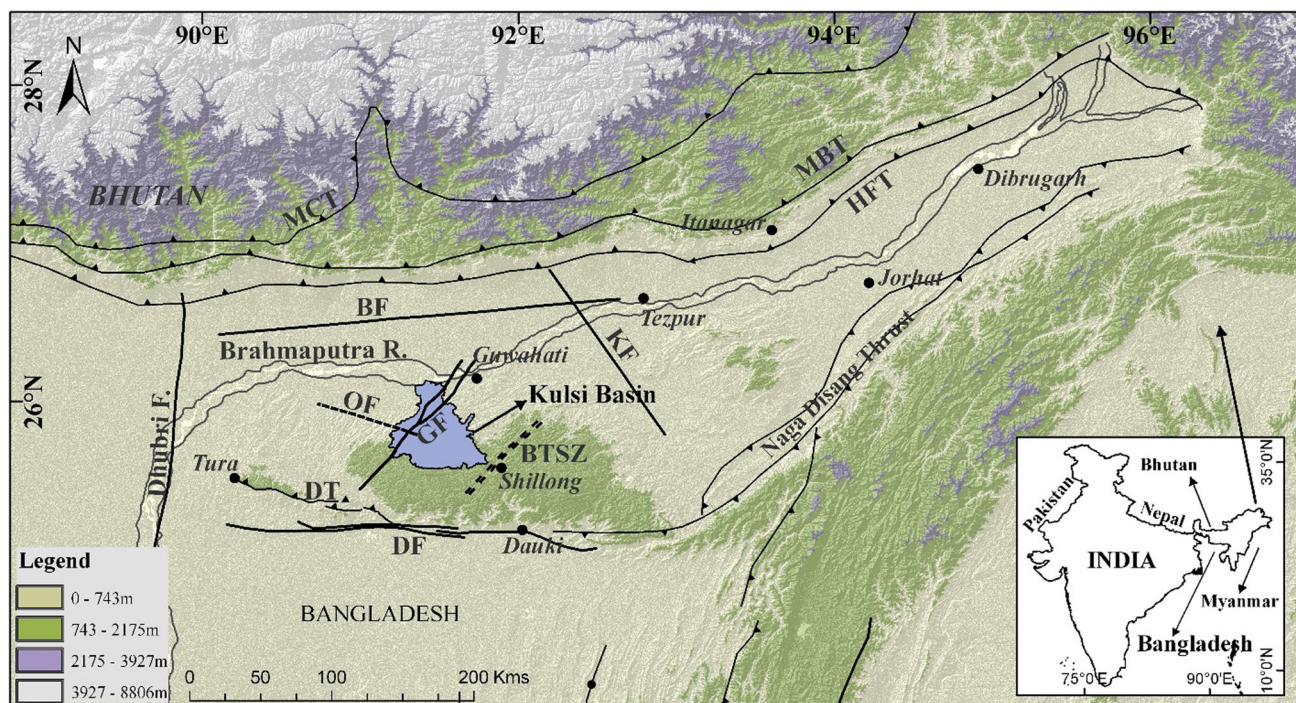


Figure 1. Relief map of northeast India with tectonic structures. Abbreviations:- MCT: Main Frontal Thrust, MBT: Main Boundary Thrust, HFT: Himalayan Frontal Thrust, BF: Brahmaputra Fault, OF: Oldham Fault, GF: Guwahati Fault, KF: Kopili Fault, BTSZ: Badapani Tyrsad Shear Zone, DT: Dapsi Thrust, DF: Dauki Fault. Map sources (Biswas and Grasemann 2005; Yin *et al.* 2010; Islam *et al.* 2011 and satellite mapping).

Fault, whereas the Naga–Disang Thrust (Schuppen Belt) as well as the sinistral strike slip Kopili Fault marks its eastern boundary (Evans 1964; Kayal *et al.* 2006). The Dhubri Fault (Gupta and Sen 1988) marks the western margin whereas the Brahmaputra Fault or the inferred Oldham Fault (Bilham and England 2001; Rajendran *et al.* 2004) delimits its northern boundary (figure 1). In addition to this, although debated there are suggestions that the SP is a pop-up structure bounded by two reverse faults (Rao and Kumar 1997; Bilham and England 2001; Rajendran *et al.* 2004). The entire plateau is dissected by several NE–SW, N–S and E–W trending structures alleged to be extensional features related to Cretaceous–Gondwana break up (Gupta and Sen 1988; Sharma *et al.* 2012) and seems to be active during the Quaternary period due to the continued north and eastward underthrusting/compression of SP (*vis-à-vis* the northeast India) against the Tibetan Plateau and Burmese Plate as evidenced by GPS data (Banerjee *et al.* 2008; Vernant *et al.* 2014). Thus, considering the tectonic setting of the SP, it is plausible to expect that the expression of cumulative seismicity would be reflected in the fluvial landforms.

Most river systems in tectonically active regions are believed to be controlled by vertical uplift

and climatic variability (Seeber and Gornitz 1983; Oberlander 1985; Burbank 1992; Zhisheng *et al.* 2001) or controlled by plate tectonics and modified by the influence of climate (Brookfield 1998). In the northeastern sub-Himalaya, fluvial geomorphological process of the Brahmaputra River Basin w.r.t channel migration, sedimentation, river bank erosion and morphotectonics has been studied in detail (Coleman 1969; Bristow 1987; Sarma 2005; Stewart *et al.* 2008; Sarma *et al.* 2015). However, such studies are scanty from other parts of the NE-Himalaya. In Arunachal Himalaya, post glacial–fluvial–aggradational process in the Kameng River and congruent deformations observed in the late-Pleistocene and mid-Holocene aggradational landforms in Siang and Dibang rivers have been considered to have formed due to enhanced tectonic uplift, whereas the role of climate remained secondary (Srivastava and Misra 2008; Luirei *et al.* 2012). In contrast, late-Pleistocene fluvial aggradation in the Teesta River valley in Sikkim NE Himalaya is attributed to changes in the climate (ISM variability) (Meetei *et al.* 2007). Meanwhile, the study of fluvial aggradational landforms pertaining to tectonics and climate from the present study area in the northern front of Shillong Plateau is absent.



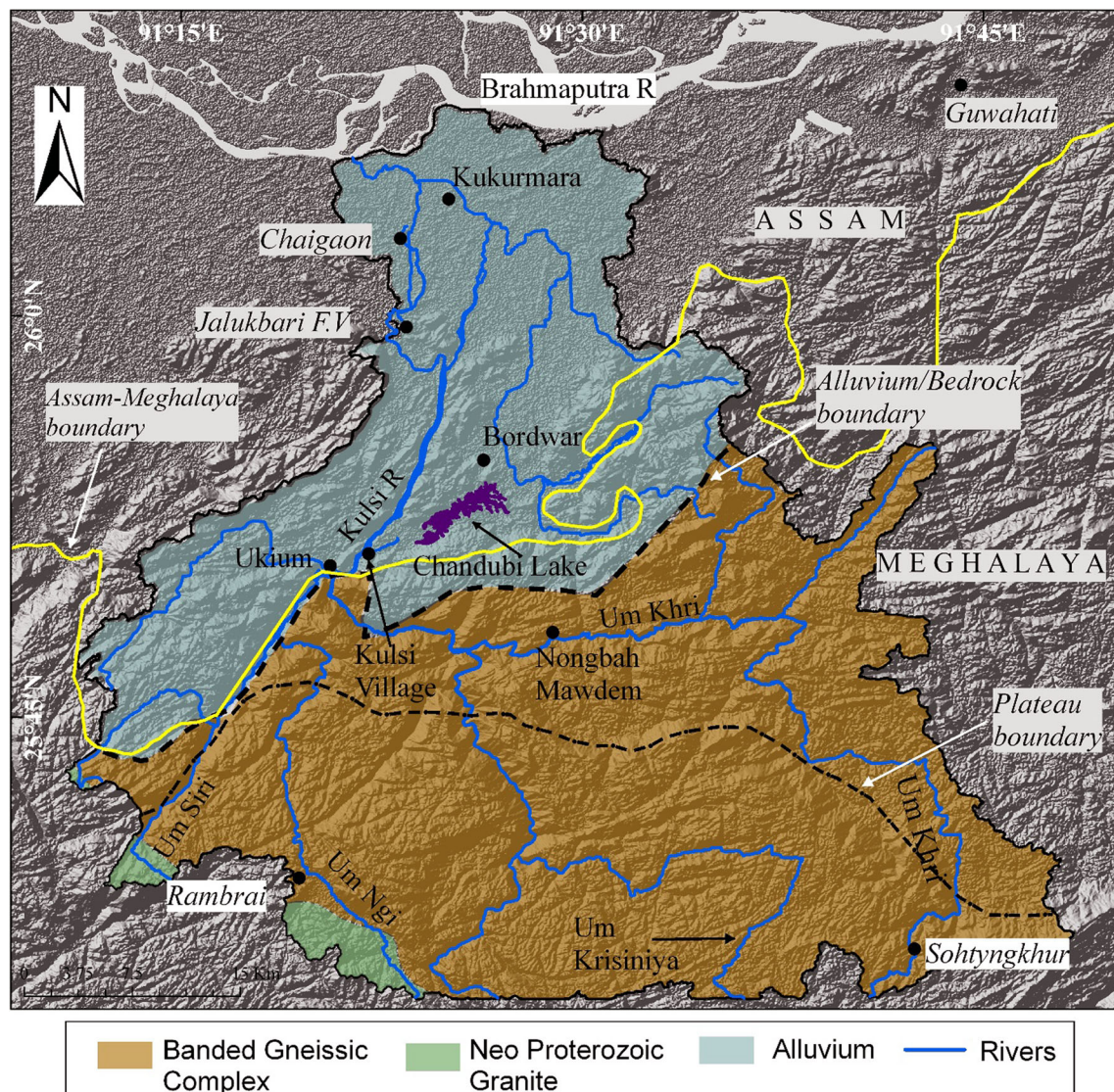


Figure 2. Study area, Kulsī River basin in the northern front of the Shillong Plateau. To the north we see the alluvium demarcating the plains of Assam, and to the south is the Banded Gneissic complex of the SP. Chandubi Lake is located in the central part of the basin.

The rivers on the sub-Himalayan region are largely influenced by the monsoon rainfall and such rivers typically experience seasonally high wavering discharge controlled by intense monsoon precipitation (Björklund 2015), which can cause abrupt change in channel course (avulsion) and large catastrophic floods (Assine 2005). The rivers of SP are likewise monsoon fed (Bookhagen *et al.* 2005; Grujic *et al.* 2006). The Kulsī River basin (figure 1, 2) in the northern front of SP is observed to demonstrate active river migration in the past as well as in the present time. This region has been described by Oldham (1898) as a fracture zone of the 1897 earthquake beginning from Bordwar

up to southwest of the Chandubi Lake where the paleochannel meets the Kulsī River (figure 2). Thus, considering that the area is tectonically active and lies in the monsoon trajectory, the present study is an attempt to understand the response of Kulsī River in terms of aggradation, incision and lateral avulsion (migration) with emphasis on the coupling between tectonics and climatic perturbations (monsoon-induced flooding). In addition to this, the Chandubi Lake contains several submerged tree trunks. Few of the submerged tree trunks are radiocarbon dated in order to ascertain the timing and factors responsible for changing hydrological conditions.

## 2. Study area

The SP is a major seismotectonic block in the northeastern India (Kayal 1987; Kayal and De 1991; Nandy and Dasgupta 1991; Rao and Kumar 1997). The major lithostratigraphic units in the SP consist of Precambrian granites and gneisses in the central and northern regions, with Cretaceous–Tertiary shelf sediments in the eastern, western and southern regions (Evans 1964; Mazumder 1976; Nandy and Dasgupta 1991). The Kulsi River in the northern front of SP is a northward flowing river system which drains into the Brahmaputra River. In the state of Meghalaya the river is known as Um Khri, whereas in Assam it is called as Kulsi. Tributary rivers such as Um Siri, Um Ngi, Um Krisiniya join Um Khri near Ukium and form Kulsi River (figure 2) which later flows into the Brahmaputra River. The Kulsi River basin has a catchment area of 2324 km<sup>2</sup>, the Um Khri–Kulsi flows ESE–WNW in the upstream segment across the hilly regions of the SP for ~40 km and then makes a westerly turn and flows for ~35 km west before it enters Assam (near Ukium) and flows NE (figure 2). The bedrocks of the drainage basin consist of Precambrian Gneissic Complex. It is suggested that the basement complex extends several kilometers north-east beneath the alluvium of the Brahmaputra (Evans 1964). The downstream section of the river (in the north) is mostly covered by alluvium. A series of N–S, NE–SW and NNE–SSW trending structures characterizes the basin where the NNE–SSW Guwahati Fault/Kulsi Fault is identified as an active fault (GSI 2000; Nandy 2001; Yin *et al.* 2010). The Chandubi Lake is located in the central part of the Kulsi River catchment, which is believed to have been formed during the 12 June 1897, Great earthquake (Oldham 1898). The lake is surrounded by natural forest and hilly terrain of the SP. The total area of the lake was around 4.48 km<sup>2</sup> with total depth of 8 m during the year 1950, but at present the area has shrunk to around 1.0 km<sup>2</sup> and the depth is reduced to around 3 m (Loharghat Forest Range office report).

## 3. Methodology

To understand the dynamics of the Kulsi River, we used digital elevation model (DEM) on GIS (Geographic Information System) platform. Lately, morphotectonic investigations using quantitative

and geostatistical topographic analysis has been widely used (Cox 1994; Chen *et al.* 2003; Duvall *et al.* 2004; Font *et al.* 2010; Imsong *et al.* 2016). Thus, quantitative channel morphometric indices such as stream longitudinal profile, stream length gradient (*SL*) index, ratio of valley floor width to valley height (*Vf*) and channel steepness (*k<sub>s</sub>*) index have been computed using Survey of India toposheets (1:50,000) and 1 arc (30 m) SRTM-DEM. Chronology of the submerged tree trunks is obtained using the conventional radio carbon dating.

### 3.1 Geomorphic indices

#### 3.1.1 Longitudinal profile and stream length gradient index (*SL*)

The longitudinal profile of a river, in general, consists of a graded concave down curve (Davis 1899; Mackin 1948; Peckham 2015). The longitudinal profile of a stream can provide clues to the underlying lithology and geologic–geomorphic history of an area (Hack 1960, 1973). Displacement or change along a graded profile (convex-up anomalies) would indicate disequilibrium due to tectonic uplift or rock-perturbations (Mackin 1948; Leopold and Maddock 1953; Whipple and Tucker 2002; Whittaker *et al.* 2007).

Stream length gradient index (*SL*) given by Hack (1973) correlates to the power of a stream to transport sediments along a stream profile. *SL* index is sensitive to changes in channel slope and has been used to detect tectonic activity by identifying anomalously high or low *SL* values on specific rock types (Keller and Pinter 2002; Chen *et al.* 2003). *SL* index is expressed as  $SL = \Delta H \times L / \Delta L$ , where  $\Delta H$  is change in elevation of the reach,  $\Delta L$  is the length of the reach and  $L$  is the total stream length from the source to the reach of interest. Recently, Font *et al.* (2010) suggested that bedrock lithology does not significantly influence the *SL* index and thus variations in *SL* values are associated with fault zones.

#### 3.1.2 Ratio of valley floor width to valley height (*Vf*)

The ratio of valley floor width to valley height (*Vf*) is measured to differentiate between broad-floored, mature and less active rivers to V-shaped valleys associated to actively uplifting/incising region. High values of *Vf* are related with low uplift rates,



Table 1. Details of Landsat satellite images used in the study.

Sensor	Date of acquisition	Bands used	Resolution
MSS	22 Nov 1972	4-6-7	60 m
MSS	24 Dec 1978	7-6-5	60 m
MSS	02 Feb 1980	7-6-5	60 m
TM	12 Dec 1991	1-4-5	30 m
TM	17 Mar 1992	1-4-5	30 m
TM	15 Nov 1993	1-4-5	30 m
TM	21 Jan 1995	1-4-5	30 m
ETM <sup>+</sup>	09 Apr 2003	8-7-6	30 m

and low values of  $Vf$  relate to high uplift rates (Bull 1977; Bull and McFadden 1977; Keller and Pinter 2002).  $Vf$  is expressed as:

$$Vf = 2Vfw / [(Eld - Esc) + (Erd - Esc)]$$

where  $Vf$  is the valley-floor width to height ratio,  $Vfw$  is the width of the valley floor,  $Eld$  and  $Erd$  are elevations of the left and right valley divides, and  $Esc$  is the elevation of the valley floor.

### 3.1.3 Channel steepness index ( $k_s$ )

Study of fluvial response to rock uplift through channel gradient and longitudinal profile by deriving quantitative estimation from topographic data has been of significant importance to understand the tectonic steadiness/unsteadiness of any particular area (Hack 1973; Kirby and Whipple 2001). As such, convexities (also known as knickpoints) are developed in a river profile in the presence of active faults which can help in identifying areas of varying rock-uplift (Hack 1957; Kirby and Whipple 2001; Whipple and Tucker 2002; Whittaker *et al.* 2007). Hence, the longitudinal profile of a stream is represented by a Power law function called channel steepness index ( $k_s$ ) in which the local channel slope ( $S$ ) is a function of the area of its upstream drainage ( $A$ ) (Hack 1957) and can be expressed as:  $S = k_s A^{-\theta}$ , where  $\theta$  is the concavity index of the river longitudinal profile. If the  $k_s$  differs at segments, then the river basin is undergoing differential uplift and *vice-versa* (Hack 1973), which can be distinguished by oversteepening of the river profiles with change in  $k_s$  (Kirby and Whipple 2001; Kirby *et al.* 2003; Tyagi *et al.* 2009). Experimentally, determined concavity values typically range between 0.35 and 0.6 (Snyder *et al.* 2000; Kirby and Whipple 2001; Roe *et al.* 2002). Considering this, we

used an intermediate value of 0.45 as suggested by Snyder *et al.* (2000) and Wobus *et al.* (2003), which is considered to be the regional mean of observed concavity values and thus the steepness values in the present study is expressed as  $k_{sn}$ . Increase in channel steepness can be manifested as an increase in rock uplift rate, and/or a decrease in erosive efficiency (Snyder *et al.* 2000; Kirby and Whipple 2001; Kirby *et al.* 2003; Duvall *et al.* 2004). However, there is no apparent relationship between channel steepness and concavity (Kirby *et al.* 2003).

## 3.2 Morphology and chronology

### 3.2.1 Morphological changes of Kuls River through satellite images

Landsat MSS, TM, ETM<sup>+</sup> of the years 1972, 1978, 1980, 1991, 1992, 1993 and 2003 (table 1) were downloaded from USGS (Earth Explorer) to analyze the temporal changes in the Kuls River morphology in its middle reach for over a period of 30 years and compared with the maximum discharge data of Kuls River for the years 1970–2000 (Brahmaputra Board, Guwahati). The remote sensing data and available maps were integrated in GIS using ArcGIS and image processing software ENVI 4.7 to map the channel morphology.

### 3.2.2 <sup>14</sup>C dating

Radiocarbon dating (or <sup>14</sup>C dating) is a method for determining the age of an object containing organic materials by using the properties of radiocarbon <sup>14</sup>C, a radioactive isotope of carbon. The method was first developed by Libby *et al.* (1949). The radiocarbon age of a sample is obtained by measurement of the residual radioactivity. Three principal isotopes of carbon

occur naturally:  $^{12}\text{C}$ ,  $^{13}\text{C}$  (both stable) and  $^{14}\text{C}$  (unstable/radioactive). These isotopes are present in the following amounts:  $^{12}\text{C}$  – 98.89%,  $^{13}\text{C}$  – 1.11% and  $^{14}\text{C}$  – 0.00000000010%. The radiocarbon method is based on the rate of decay of the radioactive carbon isotope ( $^{14}\text{C}$ ), which is formed in the upper atmosphere through the effect of cosmic ray neutrons upon nitrogen 14. The reaction is:  $14\text{N} + n \rightarrow 14\text{C} + p$  (where  $n$  is a neutron and  $p$  is a proton). The half-life of  $^{14}\text{C}$  (time it takes for half of a given amount of  $^{14}\text{C}$  to decay) is about 5,730 years. The  $^{14}\text{C}$  years does not directly equate to calendar years, because the atmospheric  $^{14}\text{C}$  concentration varies through time due to changes in the production rate, caused by geomagnetic and solar modulation of the cosmic-ray flux and the carbon cycle, hence calibration curves are adopted to record accurate ages (Reimer *et al.* 2009, 2013). The distribution of radiocarbon dates is generally described by the probability function (one standard deviation) usually represented by the Greek letter sigma ( $\sigma$ ), this holds while estimating the error. One sigma ( $1\sigma$ ) error means, that about 68% of the observations will be within one standard deviation of the experimental result, and 95% chance within  $2\sigma$  error (Bowman 1990).

Five radiocarbon dating samples were collected from submerged tree trunks in the Chandubi Lake, Assam and were dated at Birbal Sahni Institute of Paleosciences (BSIP), Lucknow, India. For radiocarbon assays, wood samples ( $\sim 100$  g) were treated with dilute (10%) HCl to remove dissolved

carbonates. Residual organic rich fractions were combusted in vacuum to obtain carbon dioxide, which was subsequently converted into benzene following standard procedures. The activity of radiocarbon was measured in a liquid scintillation counter ‘LKB-QUANTULUS’ (Yadava and Ramesh 1999). The ages are calibrated using the Calib 7.02 and IntCal 13 calibration data with  $1\sigma$  error (Reimer *et al.* 2013).

## 4. Results

### 4.1 Morphotectonic analysis

#### 4.1.1 Longitudinal profile and stream gradient (SL) analysis

The form of a river depends upon the balance between two factors: the driving forces (gravity, amount of precipitation in the drainage basin) and the resisting forces (substrate strength, friction). As such, adjustment of width and/or depth of a river is a key mechanism by which rivers respond and acts as an archive in recording landscape modification due to tectonic forcing. The longitudinal profile of Kulsi River (figure 3) is bracketed by many convexities with distinct slope breaks in the profile. In the upstream, 10 km from the source, we observe a very steep break in the profile (knick point) which is accompanied by moderately high stream gradient (figure 3). Following this, the longitudinal profile becomes moderately concave

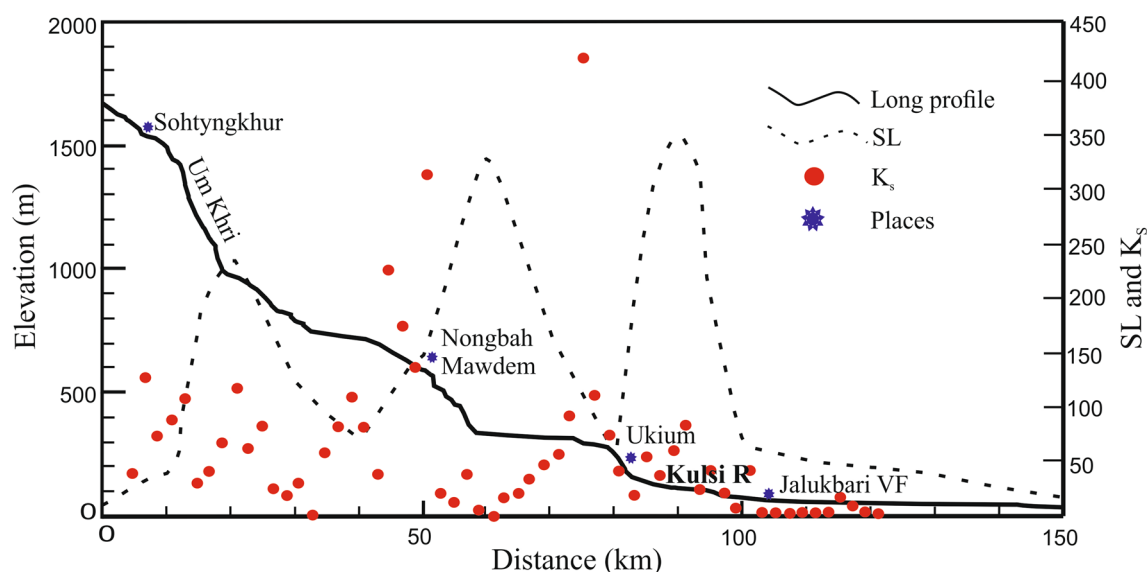


Figure 3. Longitudinal profile drawn for Kulsi River, the right panel shows the  $SL$  index (dashed line) and  $k_{sn}$  index (red dots) calculated for Kulsi River at an interval of every 2 km distance. Note that the knickpoints observed in the profile is conformable with high  $SL$  and  $k_{sn}$  indices.

for a distance of about  $\sim 30$  km. Subsequent to this, there is another steep change in the profile near Nongbah Mawdem ( $\sim 50$  km from the source) (figure 3), here we observe a high surge in the stream gradient. The profile then gradually becomes smooth for about  $\sim 20$  km downstream. Following this, we observe that the profile becomes convex associated with a break in the longitudinal profile near Ukium, which is also accompanied by anomalously high stream gradient (figure 3). The steep profiles with major slope breaks in the upstream and mid-stream section corresponds to the hilly segment of the SP dominated by bedrock, whereas from Ukium onwards, the river enters the alluvial plain section and thus the profile becomes gradually smooth downstream (figure 3).

#### 4.1.2 Channel steepness index ( $k_{sn}$ )

The channel steepness index ( $k_{sn}$ ) has been widely used in order to quantify uplifts due to tectonic inequilibrium along the longitudinal profile of a river. The average steepness index for Kulsi River is  $\leq 60$  and the values increase up to  $\leq 422$ . Based on the spatial variability of the Kulsi River, the river is broadly classified into two broad segments: (i) the upstream and mid-stream segment (dominated by bedrock) and (ii) the downstream segment (dominated by alluvium). In the upstream segment, the  $k_{sn}$  values are observed to be moderately high ( $\leq 170$ ) till  $\sim 40$  km downstream from the source, following this we observe a surge of anomalously high  $k_{sn}$  values near Nongbah Mawdem ( $k_{sn} = 225\text{--}320$ ) (figure 3). The values gradually become low ( $\leq 100$ ) for about  $\sim 20$  km downstream of Nongbah Mawdem. Subsequent to this, we observe another anomalously very high  $k_{sn}$  value ( $k_{sn} = 422$ ) at around  $\sim 75$  km from the source, and finally the  $k_{sn}$  values gradually become moderately high (around Ukium) to very low as the river enters the alluvial plains downstream of Ukium (figure 3). The very high to high  $k_{sn}$  values in the upstream and midstream along the river coincide well with knickpoints observed in the longitudinal profile of Kulsi River which is also accompanied by anomalously high stream gradients.

#### 4.1.3 Ratio of valley floor width to valley height ( $Vf$ )

The following analysis differentiates between broad floored U-shaped (stable) valleys with relatively high  $Vf$  values to V-shaped valleys with relatively

low  $Vf$  values that are actively incising commonly related to uplift. In the present study, three tectonic classes have been assigned for the  $Vf$  values calculated along the Um Khri-Kulsi River following Bull and McFadden (1977). Class 1 (tectonically active terrain) characterized by  $Vf$  values 0.1 to 1.6, class 2 (moderate to slightly active terrain) generally characterized by  $Vf$  values 1.7 to 3 and class 3 (tectonically inactive terrain) characterized by  $Vf$  values 3.4 and above. The  $Vf$  ratio calculated in the upstream segment ranges from 0.3 to 0.8, and in the mid-stream segment, the values ranges from 0.2 to 0.9. The area downstream of Ukium (figures 2, 3) has not been considered for this parameter, since the river enters the alluvial plains, it is predominantly broad floored. The  $Vf$  ratios calculated for both the segments (upstream and mid-stream) correspond to tectonic class 1 indicating tectonically active valleys.

#### 4.2 River discharge vs. lateral avulsion of Kulsi River

Avulsion is the rapid separation of a river channel to form a new channel, which is triggered usually by a flood that creates instability and causes the channel avulsion (Allen 1965; Jones and Schumm 1999; Slingerland and Smith 2004). Avulsion can be a consequence of change in peak discharge, sediment influx from tributaries, uplift or lateral tilting (tectonic), jamming of the channel through exogenous process, etc. (Miall 1996; Slingerland and Smith 1998; Jones and Schumm 1999). However, Schumm (1997) stated that until the channel approaches the avulsion threshold, even a large flood cannot cause avulsion.

Multi-temporal Landsat satellite data for the years 1972, 1978, 1980, 1991, 1993, 1995, and 2003 (table 1) were used for the identification of water bodies and to study the temporal migration of the Kulsi River. The study indicates that the location where Kulsi River enters the alluvial plain from the northern front of the SP (northeast of Ukium), the river has preferentially migrated westward (figure 4). Whereas the former course of the river was more sinuous creating channel bars, the river used to flow towards the east and turn west again to meet the river ahead of the Kulsi village. Considering that the terrain lies in a tectonically active area (Kayal 1987; Chen and Molnar 1990; Kayal *et al.* 2012) and high monsoon domain (Murata *et al.* 2007; Soja and Starkel 2007; Sato 2013), it can be suggested that the river avulsion could



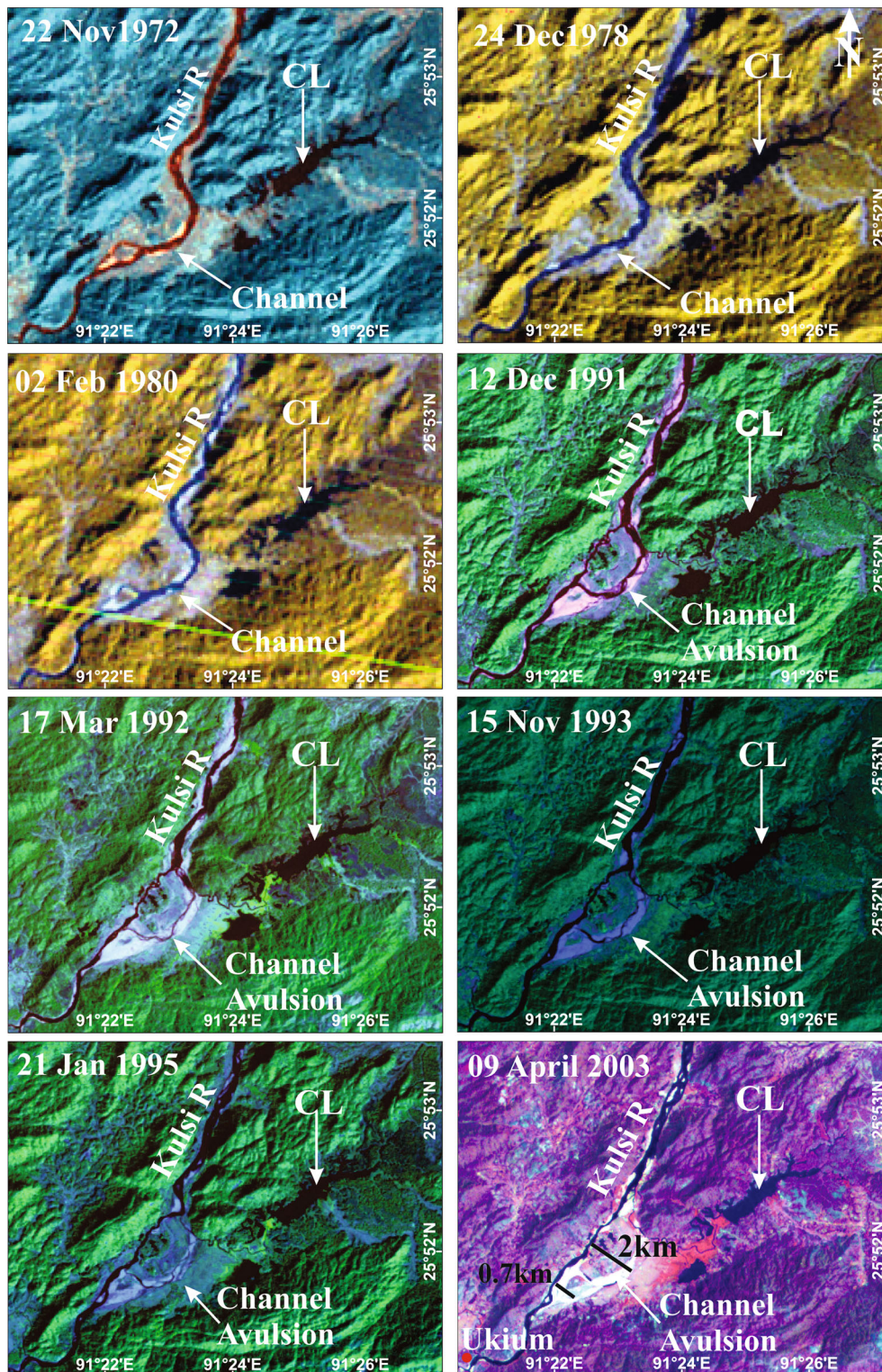


Figure 4. Multi-temporal Landsat (MSS, TM and ETM<sup>+</sup>) satellite data showing avulsion of a segment of the Kulsī River. The images show that the river was meandering into the Kulsī village with considerable sand bar as seen from data of 1972. However, during early 1980s, the river started to cut through a much straighter course and by early 1990s the river had completely abandoned its old course and started to flow through its new straight course, abandoning its paleo channel through the Chandubi Lake (CL) completely. The 2003 image marks the lateral distance of the avulsion of Kulsī River (0.7–2 km).



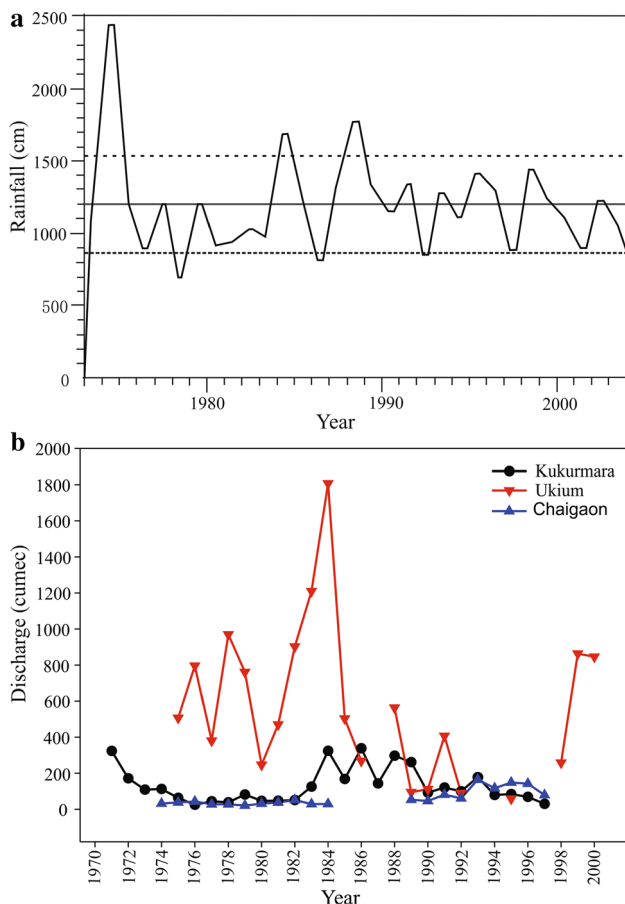


Figure 5. (a) Average rainfall data of Meghalaya (modified after Murata *et al.* (2007) for the years 1973–2000. Solid lines and dashed lines are mean and standard deviation of rainfall, respectively. (b) River discharge data of the Kulsi River at stations Ukium, Kukurmara and Chaigaon for the years 1970–2000. The data has been collected from the Brahmaputra Board, Guwahati, Assam.

be an expression of the surface deformation (tectonics) and short-term changes in the monsoon precipitation.

An average rainfall data given by Murata *et al.* (2007) (figure 5a) around the plateau indicate heavy rainfall during the period 1974, 1984, 1987–1989 and 1991. River discharge data at different stations along the Kulsi River indicate high discharge periods for the years 1975–1979, 1982–1985 and 1988 (figure 5b) which correspond well with that of the rainfall data. This data is compared with the river migration as observed in satellite data for the year 1972, 1978, 1980, 1991, 1992, 1993, 1995 and 2003 at the point where the river enters into the alluvial plains. As it can be seen during the year 1972–1980, the Kulsi River flows SW–NE and as it emerges into the plain (figure 4), the river meanders and represents a braided

channel. In 1991 image, the river had cut through a new straight channel. By 1992, the river had virtually abandoned its easterly sinuous course, migrating by about 0.7–2 km and flowing in accordance with the regional flow pattern and since then it is occupying the same course (figure 4).

#### 4.3 Morphological changes of Chandubi Lake in Kulsi River basin

The Chandubi Lake (centered at  $25^{\circ}52'48.95''$ ,  $91^{\circ}25'13.23''$ ) is located on the central part of the Kulsi catchment, where it is connected to Kulsi River by a channel on the southwestern part of the lake boundary (figure 6). According to Duarah and Phukan (2011), between the years 1911–1913 and 2002, the Chandubi Lake has shrunk in its water holding capacity from 10.23 to 1.19 km<sup>2</sup> losing 88.36% of its water spread.

Lake level fluctuations are being exceedingly used to infer the past hydrological and climatic variability (Street and Grove 1979; Vance *et al.* 1992; Morrill *et al.* 2006; Zhu *et al.* 2008). In areas that are fed by ISM, temporal changes in hydrological condition of a lake can be used to reconstruct the past changes in the strength of the ISM. The inferences towards past ISM variability are either based on (i) the lake sediment core record employing multi-proxy data such as pollen, geochemistry and isotopic studies, (ii) reconstruction of palaeo-strand line and their chronology, and (iii) spatially distributed and chronologically constrained submerged peat deposits and/or trees (Benn and Owen 1998; Chauhan *et al.* 2000, 2010; Prabhu *et al.* 2004; Morrill *et al.* 2006; Juyal *et al.* 2009; Yadav 2010; Zhisheng *et al.* 2011).

As discussed above, the Kulsi River originates from the northeastern part of the plateau and flows towards north and finally drains into the Brahmaputra River (figure 2). At the boundary between the basement rocks and the alluvial plains of the Assam valley (below Ukium, ~75 km from the headward end) (figures 2, 6), there is an abrupt widening of the river course (discussed above), which towards north-east opens into a puddle filled with rainwater that drains into the depression from the surrounding hills constituting the Chandubi Lake within the river basin. Multi-temporal satellite data of the area around Ukium (where river abruptly widens its course) (figure 4), indicate curvilinear scroll plain which shows a preferential westward migration. This implies that in the past the more eastward course of Kulsi River was

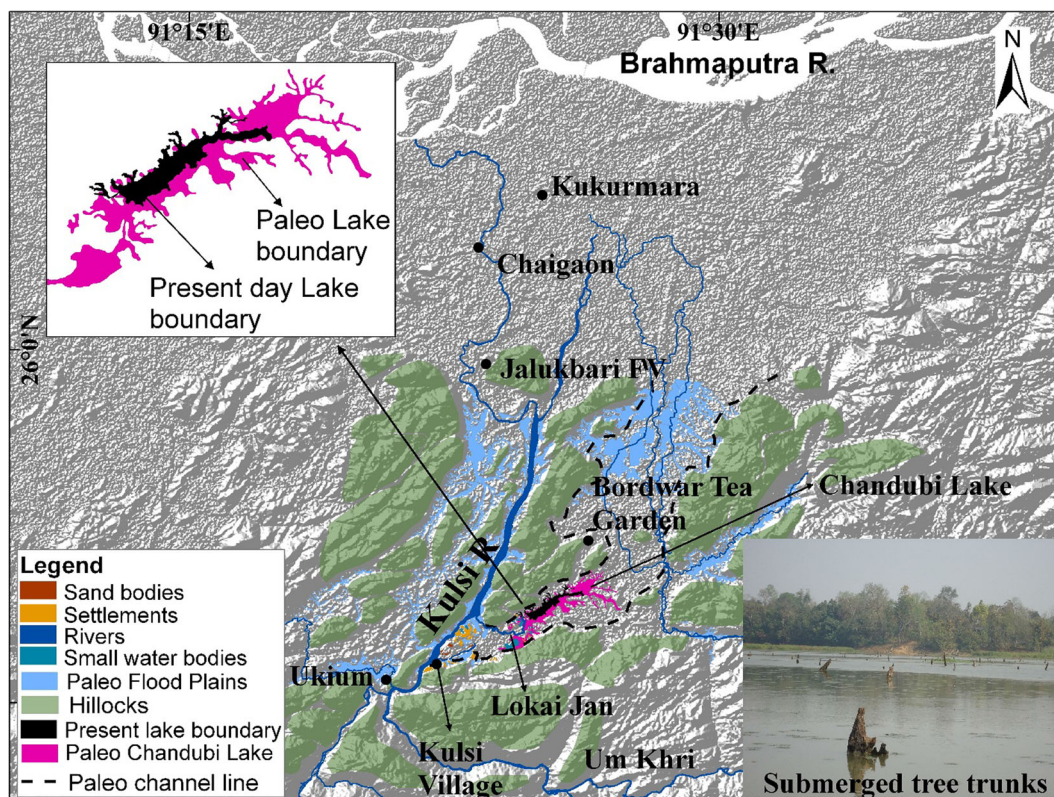


Figure 6. Geomorphology around the Chandubi Lake in Kulsī River basin. Inset figure shows the present and paleo boundary of the Chandubi Lake along with field photo of Chandubi Lake showing the location of the submerged tree trunks, samples collected for radiocarbon dating. The black dashed lines demarcate the paleo Kulsī River.

probably contributing to the hydrology of the Chandubi Lake particularly during peak flood events through subsidiary channels as observed from the paleo channel pattern of the Kulsī River in the western fringe of the lake (figure 4). Presently, the lake receives water from the surrounding catchment during the monsoon through 2nd and 3rd order streams dominantly from the southern flank of the hills (figure 6). Interestingly, the lake instead of receiving water from the river, is contributing to the river discharge through a spill-over channel known as Lokai Jan that originates from the southwestern margin of the lake and flows towards north-west (figure 6). Along this spill channel of the lake, people have extensively cultivated on the flood plain which seems to have been formed by the easterly paleo-course of the Kulsī River.

#### 4.3.1 Paleohydrological reconstruction of Chandubi Lake

In the absence of well-defined paleo strand lines along the lake margin and also no sediment core from the lake could be sampled, the present study

relied upon the nature and distribution of partially submerged tree trunks at different locations in the lake to understand the paleohydrological conditions of the Chandubi Lake. Five tree trunks are sampled for radiocarbon dating in order to ascertain their antiquity and also to evaluate the causes of the submergence. The radiocarbon ages show, one sample was too young to be dated ( $<200$  yr) whereas the remaining four are dated to be (i)  $160 \pm 50$  AD (1790 cal yr BP), (ii)  $970 \pm 50$  (980 cal yr BP) (iii)  $1190 \pm 80$  AD (760 cal yr BP) and (iv)  $1520 \pm 30$  AD (430 cal yr BP), respectively (table 2). The above ages correspond to distinct climatic events, for example, the  $160 \pm 50$  AD corresponds to the early Common Era during which the global regional climate became wetter and warmer probably equivalent to the late Holocene strengthening of ISM (Rühland *et al.* 2006). Similarly,  $970 \pm 50$  and  $1190 \pm 80$  AD broadly fall under the Medieval Warm Period (MWP) during which it has been observed both from the continental and marine records from Indian subcontinent that there was an increase in the regional temperature with concomitant increase in the ISM. The  $1520 \pm 30$  AD is proximal to the beginning of the Little Ice



Table 2. Radiocarbon dates of the submerged tree trunks, analyses of climatic variations.

Sl. no	Sample name	Age	Description
1	BS-3737, WIHG-4	160 AD $\pm$ 80 yr	The uncertainty quoted is one sigma. (To convert in BP, with 1950 being defined as today, subtract from 1950).
2	BS-3734, WIHG-3	970 yr AD $\pm$ 50 yr	
3	BS-3733, WIHG-2	1190 $\pm$ 50 yr AD	
4	BS-3738, WIHG-5	1520 AD $\pm$ 30 yr	
5	BS-3732, WIHG-1	—	The sample is dated to be modern (any age <200 yr is too young to be dated meaningfully by this method).

Age (LIA) cooling event. During this period, due to decrease in the land–sea thermal contrast, it is reasonable to assume a weakening of the insolation driven ISM. However, there are studies suggesting that LIA was episodically punctuated by short-lived warm interludes (Bradely and Jones 1993; Mann *et al.* 1998; Jones and Mann 2004; Moberg *et al.* 2005; Metcalfe *et al.* 2010; Kotlia *et al.* 2012), which may have caused increase in the ISM during LIA in context to Indian subcontinent, hence increase in precipitation (Chauhan *et al.* 2000, 2010; Gupta *et al.* 2003; Sinha *et al.* 2007).

Although the above inferences need to be further strengthened, nevertheless, the ages obtained from the submerged tree trunks indicate that the submergence of the trees were associated with periods of relatively enhanced precipitation. Given the fact that the terrain is dominated by the ISM, we suggest that the submergence of the tree trunks were associated with phases of enhanced ISM.

## 5. Discussion

### 5.1 Morphotectonic implications

Geomorphic parameters have been widely used to identify landscapes that are undergoing tectonic instability (Burbank and Anderson 2001; Keller and Pinter 2002; Goudie *et al.* 2005). Towards this, fluvial landforms are considered as one of the sensitive recorder of crustal deformation (tectonics). The reason being on multi-millennial time scales tectonics, lithology and climate imparts first order control in determining patterns of fluvial activity over time (Davis 1899; Duvall *et al.* 2004; Whitaker *et al.* 2007).

The Kulsi River flows through an almost E–W trending escarpment which demarcates the boundary between the Shillong Plateau and the alluvial plains of Assam. The river flows through two different lithologies, *viz.*, through the Banded Gneissic Complex of the Shillong Plateau in the

upstream forming narrow valleys and the Assam alluvial plains in the downstream where the river has carved wide valleys showing evidence of paleo river channels. The longitudinal river profile analysis along with stream gradient indices, shows major slope breaks (knickpoints) with short wavelength convexities coupled with abnormally very high stream gradient indices. According to Troiani and Seta (2008), peak *SL* values with short wavelength convexities in river profiles occur either at significant lithological changes and/or at fault outcrops. In the upstream segment (figure 3), we observe a prominent break in the slope accompanied by moderately high *SL* peak. Subsequent to this in the midstream segment, we observe two slope breaks, one near Nongbah Mawdem and the second near Ukium accompanied by very high *SL* peaks (figure 3). The former two slope breaks do not correspond to any lithological change, whereas the third (near Ukium) corresponds with the lithological boundary between the Banded Gneissic Complex of the Shillong Plateau and the alluvial plains of Assam.

The geomorphic indices suggest that the former (two) slope breaks are due to a fault passing along the river course which we assume is due to the Guwahati Fault (Yin *et al.* 2010) that passes along the Kulsi River; this is also supported by high to very high  $k_{sn}$  values along with very low  $V_f$  values calculated in the upstream and midstream segments. Very high and high  $k_{sn}$  values in the upstream and midstream segments of the river correspond well with the knickpoints observed in the Kulsi River profile and associated high *SL* indices (figure 3), thus implying that the tectonic activity in the area is outpacing erosion.

### 5.2 Climatic implications

River migration is not uncommon in a transitional zone that is between the high relief mountainous topography and low relief alluvial plain (as in

the present case). The paleo-course of the Kulsi River, inferred based on satellite imagery shows that at the downstream of the transitional zone ( $\sim 2.7$  km downstream of Ukium), the river used to flow through a U-shaped easterly linear track that has innumerable relict channel bar implying lateral migration ranging (in length) from 0.7 to 2 km westward till 1991 (figure 4). The relict course appears to feed the Chandubi Lake during peak floods. The Kulsi River discharge data from Ukium station located at Ukium ( $25^{\circ}50.690'N$ ,  $91^{\circ}20.569'E$ ), indicate high water discharges during the years 1975–1979, 1982–1985 and 1988 which correspond well with the precipitation data for the same period (figure 5a). Correspondingly, as discussed above, the Guwahati Fault passes along the Kulsi River, and as such it is possible to assume that the activity along the fault in the Kulsi River catchment has resulted in shearing and fracturing of the catchment lithology, implying that the Kulsi catchment is a transport limited system. Therefore, the river avulsion can be attributed to the increase in sediment supply associated with high rainfall event/high river discharge during the year 1984 and the following years. Although in the succeeding years this region experienced high discharge, the threshold sediment flux clogging the sinuous course was achieved during 1984. This would imply that, although, in a terrain which is tectonically active, the river can migrate laterally purely due to threshold perturbation caused due to unusual weather event, which in the present case is attributed to the 1984 high rainfall, thus the avulsion of the Kulsi River is attributed to inconsistent climatic fluctuations.

Furthermore, hydrological changes in the Chandubi Lake inferred through river discharge data and  $^{14}C$  analysis on the submerged tree trunks suggest that the lake have been periodically flooded in the past causing the submergence of the tree trunks. The  $160 \pm 50$  AD age obtained on submerged tree trunk indicate a period corresponding to the late Holocene strengthening of ISM (Rühland *et al.* 2006),  $970 \pm 50$  and  $1190 \pm 80$  AD represents the Medieval Warm Period (WMP) (Metcalfe *et al.* 2010), and  $1520 \pm 30$  AD is close to the beginning of the Little Ice Age (LIA) (Bradely and Jones 1993; Kotlia *et al.* 2012). Our study suggests that three major climatic excursions of enhanced ISM are well represented by increased water level in the Chandubi Lake. The study is important as it indicates the sensitivity of the monsoon-dominated

eastern Himalayan foothills towards short-term global paleo-climatic perturbations which lasted for few centuries. This implies that the climate (ISM) of the eastern Himalaya is coupled with the global climatic phenomenon.

## 6. Conclusions

Based on detailed morphometry and geomorphic indices of Kulsi River along with satellite image analysis on the movement of the river and chronology of the tree trunks obtained from the Chandubi Lake (in the Kulsi River catchment) allows us to draw the following inferences.

- The northern part of the Shillong Plateau is neotectonically active as evidenced by the morphometric parameters such as river longitudinal profile, *SL* index, channel steepness index ( $k_{sn}$ ) and *Vf* ratio analyzed for Kulsi River catchment.
- The sinuous course in the middle reach of the Kulsi River began to clog due to high sediment flux coupled with high rainfall events during 1984, 1985 and early 1990's that led to the 0.7–2 km westward migration of the Kulsi River in its middle course, as a result the river gradually occupied a rather straighter course by 1991.
- The radiocarbon chronology of the submerged tree trunks suggests relatively high lake levels in Chandubi Lake that was routed through the high fluvial discharge of Kulsi River during relatively strengthened ISM particularly during the Late Holocene, Medieval Warm period and during the beginning of Little Ice Age.
- Our analysis calls for more detailed investigations to understand the mechanism of coupled neotectonic and paleo-climatic processes towards landform evolution in climatically and tectonically sensitive areas such as the northeastern Himalaya.

## Acknowledgements

This study is part of WI's Ph.D thesis. WI acknowledges Council of Scientific and Industrial Research, HRDG New Delhi for SRF-NET fellowship (file no: 09/420/(0002)/2012-EMR-I). The authors are thankful to Wadia Institute of Himalayan Geology, Dehardun and Gauhati University, Assam for research facilities. WI is also thankful to Mr. Atul Sarma, Executive Engineer, Brahmaputra Board, Guwahati for providing river discharge data on



Kulsi River and Mr. K K Deka, Forest Range Officer, Loharghat Forest Reserve for providing official reports on Chandubi Lake. The authors are also thankful to the two anonymous reviewers who helped to improve the manuscript substantially.

## References

- Allen J R L 1965 A review of the origin and characteristics of recent alluvial sediments; *Sedimentology* **5** 89–191.
- An Yin, Dubey C S, Webb A A G, Kelty T K, Grove M, Gehrels G E and Burgess W P 2010a Geologic correlation of the Himalayan orogen and Indian craton: Part 1. Structural geology, U–Pb zircon geochronology and tectonic evolution of the Shillong Plateau and its neighboring regions in NE India; *Geol. Soc. Am. Bull.* **122** 336–359.
- Assine M L 2005 River avulsions on the Taquari mega fan, Pantanal wetland, Brazil; *Geomorphology* **70**(3–4) 357–371.
- Banerjee P, Bürgmann R, Nagarajan B and Apel E 2008 Intraplate deformation of the Indian subcontinent; *Geophys. Res. Lett.* **35** L18301, <https://doi.org/10.1029/2008GL035468>.
- Benn D I and Owen L A 1998 The role of the Indian Summer Monsoon and the mid-latitude westerlies in Himalayan glaciation: Review and speculative discussion; *J. Geol. Soc.* **155**(2) 353–363.
- Bilham R and England P 2001 Plateau pop-up during the great 1897 Assam earthquake; *Nature* **410** 806–809.
- Biswas S and Grasemann B 2005 Quantitative morphotectonics of the southern Shillong Plateau (Bangladesh/India); *Austr. Earth Sci.* **97** 82–93.
- Björklund P P 2015 Morphodynamics of rivers strongly affected by monsoon precipitation: Review of depositional style and forcing factors; *Sedim. Geol.* **323** 110–147.
- Bookhagen B, Thiede R C and Strecker M R 2005 Abnormal monsoon years and their control on erosion and sediment flux in the high, arid northwest Himalaya; *Earth Planet. Sci. Lett.* **231**(1) 131–146.
- Bowman S 1990 *Radiocarbon dating*; Univ. of California Press.
- Bradely R S and Jones P D 1993 ‘Little Ice Age’ summer temperature variations: Their nature and relevance to recent global warming trend; *Holocene* **3**(4) 367–376.
- Bristow C S 1987 Brahmaputra River: Channel migration and deposition; In: Recent Developments in Fluvial Sedimentology (eds) Ethridge F G, Flores R M and Harvey M D, *Soc. Econ. Palaeontol. Mineral. Spec. Publ.* **39** 63–74.
- Brookfield M E 1998 The evolution of the great river systems of southern Asia during the Cenozoic India–Asia collision: Rivers draining southwards; *Geomorphology* **22**(3–4) 285–312.
- Bull W B 1977 Tectonic geomorphology of the Mojave Desert, California: U.S. Geological Survey contract report, 14-08-001-G-394; Office of Earthquakes, Volcanoes, and Engineering, Menlo Park, California, 188p.
- Bull W B and McFadden L D 1977 Tectonic geomorphology north and south of the Garlock fault, California; In: *Geomorphology in arid regions* (ed.) Doehring D O, State University of New York at Binghamton, pp. 115–138.
- Burbank D W 1992 Causes of recent Himalayan uplift deduced from deposited patterns in the Ganges basin; *Nature* **357** 680–683.
- Burbank D W and Anderson R S 2001 *Tectonic Geomorphology*; 1st edn, Blackwell Science Ltd.
- Chauhan M S, Mazari R K and Rajagopala G 2000 Vegetation and climate in upper Spiti region, Himachal Pradesh during late Holocene; *Curr. Sci.* **79**(3) 373–377.
- Chauhan O S, Vogelsang E, Basavaiah N and Abdul K U S 2010 Reconstruction of the variability of SW monsoon during the past 3 Ka from the continental margin of the south-eastern Arabian Sea; *J. Quat. Sci.* **25**(6) 798–807.
- Chen W P and Molnar P 1990 Source parameters of earthquakes and intraplate deformation beneath the Shillong Plateau and the northern Indo-Burman Ranges; *J. Geophys. Res.* **95**(B8) 12527–12552.
- Chen Y C, Sung Q and Cheng K Yu 2003 Along-strike variations of morphotectonic features in the western foothills of Taiwan: Tectonic implications based on stream-gradient and hypsometric analysis; *Geomorphology* **56** 109–137.
- Coleman J M 1969 Brahmaputra River: Channel processes and sedimentation; *Sedim. Geol.* **3**(2–3) 129–239.
- Cox T 1994 Analysis of drainage-basin symmetry as a rapid technique to identify areas of possible Quaternary tilt-block tectonics: An example from the Mississippi Embayment; *Geol. Soc. Am. Bull.* **106** 571–581.
- Dasgupta S 2011 Earthquake geology, geomorphology and hazard scenario in northeast India: Appraisal; National workshop on Earthquake risk mitigation strategy in northeast, February 24–25, Guwahati Assam, pp. 24–39.
- Davis M 1899 The geographical cycle; *Geograph. J.* **14**(5) 481–504.
- Duarah B P and Phukan S 2011 Understanding the tectonic behaviour of Shillong Plateau, India using remote sensing data; *Geol. Soc. India* **77** 105–112.
- Duvall A, Kirby E and Burbank D 2004 Tectonic and lithologic controls on bedrock channel profiles and process in coastal California; *J. Geophys. Res.* **109** F03002.
- England P and Bilham R 2015 The Shillong Plateau and the great 1897 Assam earthquake; *Tectonics* **34**(9) 1792–1812.
- Evans P 1964 The tectonic framework of Assam; *Geol. Soc. India* **5** 80–96.
- Font M, Amorese D and Lagrade J L 2010 DEM and GIS analysis of the stream gradient index to evaluate effects of tectonics: The Normandy intraplate area (NW France); *Geomorphology* **119** 172–180.
- Geological Survey of India (GSI) 2000 Seismotectonic Atlas.
- Goudie A, Anderson M, Burt T, Lewin J, Richards K, Whalley B and Worsely P 2005 *Geomorphological Techniques*; 2nd edn, Routledge, Taylor and Francis, pp. 49–107.
- Grujic D, Coutand I, Bookhagen B, Bonnet S, Blythe A and Duncan C 2006 Climatic forcing of erosion, landscape, and tectonics in the Bhutan Himalayas; *Geology* **34**(10) 801–804.
- Gupta A K, Anderson D M and Overpeck J T 2003 Abrupt changes in the Asian southwest monsoon during the Holocene and their links to the North Atlantic Ocean; *Nature* **421** 354–357.

- Gupta R P and Sen A K 1988 Imprints of the Ninety-East ridge in the Shillong Plateau, Indian Shield; *Tectonophysics*. **154** 335–341.
- Hack J T 1957 Studies of longitudinal stream profiles in Virginia and Maryland; *Geol. Surv. Prof. Paper* **294-B** 45–97.
- Hack J T 1960 Interpretation of erosional topography in humid temperate regions; *Am. J. Sci.* **258** 80–97.
- Hack J T 1973 Stream profile analysis and stream gradient Index; *J. Res. US Geol. Survey* **1(4)** 421–429.
- Imson W, Choudhury S and Phukan S 2016 Ascertaining the neotectonic activities in the southern part of Shillong Plateau through geomorphic parameters and remote sensing data; *Curr. Sci.* **110** 91–98.
- Islam M S, Ryuichi S and Kayal J R 2011 Pop-up tectonics of the Shillong Plateau in northeastern India: Insight from numerical simulations; *Gondwana Res.*, <https://doi.org/10.1016/j.gr.2010.11.007>.
- Jones L S and Schumm S A 1999 Causes of avulsion: An overview; *Spec. Publ. Int. Assoc. Sedimentol.* **28** 171–178.
- Jones P D and Mann M E 2004 Climate over past Millennia; *Rev. Geophys.* **42** RG2002.
- Juyal N, Pant R K, Basavaiah N, Bhushan R, Jain M, Saini N K, Yadava M G and Singhvi A K 2009 Reconstruction of last Glacial to early Holocene monsoon variability from relict lake sediments of the Higher Central Himalaya, Uttarakhand, India; *J. Asian Earth Sci.* **34** 437–449.
- Kayal J R 1987 Microseismicity and source mechanism study: Shillong Plateau, northeast India; *Bull. Seismol. Soc. Am.* **77** 184–194.
- Kayal J R and De R 1991 Microseismicity and tectonic in northeast India; *Bull. Seismol. Soc. Am.* **81(1)** 131–138.
- Kayal J R, Arefiev S S, Barua S, Hazarika D, Gogoi N, Gautam J L, Baruah S, Dorbath C and Tatevossian R 2012 Large and great earthquakes in the Shillong Plateau–Assam valley area of northeast India region: Pop-up and transverse tectonics; *Tectonophysics*. **532** 186–192.
- Kayal J R, Arefiev S S, Barua S, Hazarika D, Gogoi N, Kumar A, Chowdhury S N and Kalita S 2006 Shillong Plateau earthquakes in the northeast India region: Complex tectonic model; *Curr. Sci.* **91(1)** 109–114.
- Keller E A and Pinter N 2002 *Active Tectonics: Earthquake, Uplift, and Landscape*; 2nd edn, Prentice Hall, Englewood Cliffs, pp. 121–147.
- Kirby E and Whipple K X 2001 Quantifying differential rock uplift rates via stream profile analysis; *Geol. Soc. Am.* **29(5)** 415–418.
- Kirby E, Whipple K X, Tang W and Chen Z 2003 Distribution of active rock uplift along the eastern margin of the Tibetan Plateau: Inferences from bedrock channel longitudinal profiles; *J. Geophys. Res.* **108(B4)** 2217.
- Kotlia B S, Ahmad S M, Zhao J X, Raza W, Collerson K D, Joshi L M and Sanwal J 2012 Climatic fluctuations during the LIA and post-LIA in the Kumaun Lesser Himalaya, India: Evidence from a 400 yr old stalagmite record; *Quat. Int.*, <https://doi.org/10.1016/j.quaint.2012.01.025>.
- Leopold L B and Maddock T Jr 1953 The hydraulic geometry of stream channels and some physiographic implications; *Geol. Surv. Prof. Paper* 252.
- Libby W F, Anderson E C and Arnold J R 1949 Age determination by radiocarbon content: World-wide assay of natural radiocarbon; *Science* **109(2827)** 227–228.
- Luirei K, Bhakuni S S, Srivastava P and Suresh N 2012 Late Pleistocene–Holocene tectonic activities in the frontal part of NE Himalaya between Siang and Dibang river valleys, Arunachal Pradesh, India; *Zeitschrift für Geomorphologie* **56(4)** 477–493.
- Mackin H J 1948 Concept of the graded river; *Geol. Soc. Am.* **55** 463–512.
- Mann M E, Bradley R S and Hughes M K 1998 Global-scale temperature patterns and climate forcing over the past six centuries; *Nature* **392** 779–787.
- Mazumder S K 1976 A summary of the Precambrian geology of the Khasi Hills, Meghalaya; *Geol. Surv. India, Misc. Publ.* **23**.
- Meetei L I, Pattanayak S K, Bhaskar A, Pandit M K and Tandon S K 2007 Climatic imprints in Quaternary valley fill deposits of the middle Teesta valley, Sikkim Himalaya; *Quat. Int.* **159** 32–46.
- Metcalfe S E, Jones M D, Davies S J, Noren A and MacKenzie A 2010 Climate variability over the last two millennia in the North American monsoon region, record in laminated lake sediments from Laguna de Juanacatlan, Mexico; *Holocene* **20(8)** 1195–1206.
- Miall A D 1996 *The Geology of fluvial deposits*; Springer-Verlag, Berlin.
- Moberg A, Sonechkin D M, Holmgren K, Datsenko N M and Karlen W 2005 Highly variable Northern Hemisphere temperatures reconstructed from low- and high- resolution proxy data; *Nature* **433** 613–617.
- Morrill C, Overpeck J T, Cole J E, Liu K, Shen C and Tang L 2006 Holocene variations in the Asian monsoon inferred from the geochemistry of lake sediments in central Tibet; *Quat. Res.* **65** 232–243.
- Murata F, Hayashi T, Matsumoto J and Asada H 2007 Rainfall on the Meghalaya Plateau in the northeastern India – one of the rainiest places in the world; *Nat. Hazards* **42** 391–399.
- Nandy D R 2001 *Geodynamics of northeastern India and the adjoining region*; ACB Publications.
- Nandy D R and Dasgupta S 1991 Seismotectonic domains of northeastern India and adjacent areas; *Phys. Chem. Earth* **18** 371–384.
- Oberlander T M 1985 Origin of drainage transverse to structures in orogeny; *Tectonic Geomorph.*, pp. 155–182.
- Oldham R D 1898 General Report – The earthquake of 12<sup>th</sup> June 1897; *Asiat. Misc.* **2** 16–18.
- Peckham S D 2015 Longitudinal elevation profiles of rivers: Curve fitting with functions predicted by theory; In: *Geomorphometry for Geosciences* (eds) Jasiewicz J, Zwolinski Zb, Mitasova H and Hengl T, *Int. Soc. Geomorphometry*, Poland, pp. 137–140.
- Prabhu C N, Shankar R, Anupama K, Taieb M, Bonnefille R, Vidal L and Prasad S 2004 A 200-Ka pollen and oxygen – isotopic record from two sediment cores from the eastern Arabian Sea; *Paleogeogr. Paleoclimatol. Paleoecol.* **214** 309–321.
- Rühland K, Phadtare N R, Pant R K, Sangode S J and Smol J P 2006 Accelerated melting of Himalayan snow and ice triggers pronounced changes in a valley peatland from northern India; *Geophys. Res. Lett.* **33** L15709.
- Rajendran C P, Rajendran K, Duarah B P, Baruah S and Earnest A 2004 Interpreting the style of faulting and pale-



- oseismicity associated with the 1897 Shillong, northeast India, earthquake: Implications for regional tectonism; *Tectonics* **23** TC4009.
- Rao N P and Kumar M R 1997 Uplift and tectonics of the Shillong Plateau, northeast India; *J. Phys. Earth* **45** 167–176.
- Reimer P J, Baillie M G L, Bard E, Bayliss A, Beck J W, Blackwell P G, Bronk R C, Buck C E, Burr G S, Edwards R L, Friedrich M, Grootes P M, Guilderson T P, Hajdas I, Heaton T J, Hogg A G, Hughen K A, Kaiser K F, Kromer B, McCormac F G, Manning S W, Reimer R W, Richards D A, Southon J R, Talamo S, Turney C S M, van der Plicht J and Weyhenmeyer C E 2009 IntCal09 and Marine09 radiocarbon age calibration curves, 0–50,000 years cal BP; *Radiocarbon* **51**(4) 1111–1150.
- Reimer P J, Bard E, Bayliss A and Beck J W 2013 IntCal13 and Marine13 radiocarbon age calibration curves 0–50,000 years cal BP; *Radiocarbon* **55**(4) 1869–1887.
- Roe G H, Montgomery D R and Hallet B 2002 Effects of orographic precipitation variations on the concavity of steady-state river profiles; *Geology* **30**(2) 143–146.
- Sarma J N 2005 Fluvial process and morphology of the Brahmaputra River in Assam, India; *Geomorphology* **70** 226–256.
- Sarma J N, Acharjee S, Murgante B 2015 Morphotectonic study of the Brahmaputra basin using geoinformatics; *J. Geol. Soc. of India* **86** 324–330.
- Sato T 2013 Mechanism of orographic precipitation around the Meghalaya Plateau associated with intra-seasonal oscillation and the diurnal cycle; *Mon. Wea. Rev.* **141**(7) 2451–2466.
- Schumm S A 1977 *The Fluvial System*; John Wiley & Sons, New York.
- Seeber L and Gornitz V 1983 River profiles along the Himalayan arc as indicators of active tectonics; *Tectonophys.* **92** 335–367.
- Sharma R, Gouda H C, Singh R K and Nagaraju B V 2012 Structural study of Meghalaya Plateau through aeromagnetic data; *J. Geol. Soc. India* **79** 11–29.
- Sinha A, Cannariato K G, Stott L D, Cheng H, Edwards R L, Yadav M G, Ramesh R and Singh I B 2007 A 900-year (600 to 1500 AD) record of the Indian summer monsoon precipitation from the core monsoon zone of India; *Geophys. Res. Lett.* **34** L16707.
- Slingerland R and Smith N D 1998 Necessary conditions for a meandering-river avulsion; *Geology* **26**(5) 435–438.
- Slingerland R and Smith N D 2004 River avulsions and their deposits; *Earth Planet. Sci. Lett.* **32** 257–285.
- Snyder N P, Whipple K X, Tucker G E and Merritts D J 2000 Landscape response to tectonic forcing: Digital elevation model analysis of stream profiles in the Medocino triple junction region, northern California; *Geol. Geol. Surv. Am. Bull.* **112**(8) 1250–1263.
- Soja R and Starkel L 2007 Extreme rainfalls in eastern Himalaya and southern slope of Meghalaya Plateau and their geomorphologic impacts; *Geomorphology* **84** 170–180.
- Srivastava P and Misra D K 2008 Morpho-sedimentary records of active tectonics at the Kameng River exit, NE Himalaya; *Geomorphology* **97** 187–198.
- Stewart R J, Hallet B, Zeitler P K, Malloy M A, Allen C M and Trippett C 2008 Brahmaputra sediment flux dominated by highly localized rapid erosion from the easternmost Himalaya; *Geol. Soc. Am.* **36**(9) 711–714.
- Street F A and Grove A T 1979 Global maps of lake-level fluctuations since 30,000 yr B.P.; *Quat. Res.* **12** 83–118.
- Troiani F and Seta D M 2008 The use of the stream length-gradient index in morphotectonic analysis of small catchments: A case study from central Italy; *Geomorphology* **102** 159–168.
- Tyagi A K, Chaudhary S, Rana N, Sati S P and Juyal N 2009 Identifying areas of differential uplift using steepness index in the Alaknanda basin, Garhwal Himalaya, Uttarakhand; *Curr. Sci.* **97**(10) 1473–1477.
- Vance R E, Mathews R W and Clague J J 1992 7000-year record of lake-level change on the northern Great Plains: A high-resolution proxy of past climate; *Geology* **20** 879–882.
- Vernant P, Bilham R, Szeliga W, Drupka D, Kalita S, Bhattacharyya A K, Gaur V K, Pelgay P, Cattin R and Berthet T 2014 Clockwise rotation of the Brahmaputra Valley relative to India: Tectonic convergence in the eastern Himalaya, Naga Hills, and Shillong Plateau; *J. Geophys. Res. Solid Earth* **119**(8) 6558–6571.
- Whipple K and Tucker G 2002 Implications of sediment-flux dependent river incision models for landscape evolution; *J. Geophys. Res.* **107**, <https://doi.org/10.1029/2000JB000044>.
- Whittaker A C, Cowie P A, Attal M, Tucker G E and Roberts G P 2007 Bedrock channel adjustment to tectonic forcing: Implications for predicting river incision rates; *Geol. Soc. Am.* **35**(2) 103–106.
- Wobus WC, Hodges K V and Whipple K X 2003 Has focused denudation sustained active thrusting at the Himalayan topography front?; *Geol. Soc. Am.* **31**(10) 861–864.
- Yadav R R 2010 Long-term hydro climatic variability in monsoon shadow zone of western Himalaya, India; *Clim. Dyn.*, <https://doi.org/10.1007/s00382-010-0800-8>.
- Zhisheng A, Clemens S C, Shen J, Qiang X, Zhangdong J, Sun Y, Prell W L, Luo J, Wang S, Xu H, Cai Y, Zhou W, Liu X, Liu W, Shi Z, Yan L, Xiao X, Chang H, Wu F, AI Li and Lu F 2011 Glacial-interglacial Indian summer monsoon dynamics; *Science* **333** 719–723.
- Zhisheng An, Kutzbach J E, Prell W L and Porter S C 2001 Evolution of Asian monsoon and phased uplift of the Himalayan–Tibetan Plateau since late Miocene times; *Nature* **411** 62–66.
- Zhu L, Zhen X, Wang J, Lü H, Kitagawa H and Possnert G 2008 A ~30,000-year record of environmental changes inferred from Lake Chen Co, southern Tibet; *J. Paleolimnol.* **42** 343–358.